Dynamics and dispersion in Eulerian-Eulerian DNS of two-phase flows

By A. Kaufmann †, O. Simonin ‡, T. Poinsot †, AND J. Helie ‡

A DNS approach for Eulerian-Eulerian dispersed two-phase flows is tested. The need for a subgrid stress term in the dispersed phase momentum equation is identified and a simple model for this stress term allows the calculation of an experimental test case with inertial particles in homogeneous turbulence. Results are compared to Eulerian-Lagrangian simulations.

1. Introduction and motivation

Particle-laden flows are of great interest since they occur in a variety of industrial applications. Knowledge of particle transport and concentration properties are crucial for the design of such applications. Numerical simulations coupling Lagrangian tracking of discrete particles with DNS of the carrier-phase turbulence provide a powerful tool to investigate such flows. When particle numbers become large, particle-particle and turbulence modification effects become important and such numerical simulations have the drawback of being numerically expensive. Numerical simulations based on separate Eulerian balance equations for both phases, coupled through inter-phase exchange terms, might be an alternative approach in such cases. Such Eulerian-Eulerian DNS approach has been validated for the case of particles with low inertia which follow the carrier fluid flow almost instantaneously due to their small response time compared to the integral time scales of the turbulence (Druzhini & Elghobashi (1999)).

In the case of inertial particles, with response times comparable to the integral time scales, additional effects have to be taken into account. Indeed, as pointed out by Février (2000) and Février *et al.* (2002), particle phase transport equations must account for dispersion effects due to a local random motion which is induced by particle-turbulence and particle-particle interactions. Following Février *et al.* (2002), a conditional average of the dispersed phase with respect to the carrier phase flow realization allows the derivation of instantaneous mesoscopic particle fields and instantaneous Eulerian balance equations accounting for the effect of random motion. From forced isotropic turbulence simulations, Février *et al.* (2002) showed that the uncorrelated, quasi-Brownian motion of the particles increases with inertia (high Stokes numbers). In cases such that the particle relaxation time is comparable to the Lagrangian integral time scale, the kinetic energy of quasi-Brownian motion is about 30% of the total kinetic energy of the dispersed phase.

The importance of quasi-Brownian motion (QBM) is illustrated in a preliminary test case of decaying homogeneous isotropic turbulence. The Eulerian model is then applied to the experimental case of Snyder & Lumley (1971) which has previously been simulated by Elghobashi & Truesdell (1992) using a Lagrangian approach. This allows the present Eulerian simulation to be compared to experiment and Lagrangian simulation.

† CERFACS, 42 Av. G. Coriolis, 31057 Toulouse, France
‡ IMFT, Av. C. Soula, 31400 Toulouse, France

2. The Eulerian model

Eulerian equations for the dispersed phase may be derived by several means. A popular simple way consists of volume filtering of the the separate, local, instantaneous phase equations accounting for the interfacial jump conditions (Druzhini & Elghobashi (1999)). Such an averaging approach is very restrictive, because particle size and particle distance have to be smaller then the smallest length scale of the turbulence.

A different, not totally equivalent way is the statistical approach in the framework of kinetic theory. In analogy to the derivation of the Navier-Stokes equations by non-equilibrium statistics (Chapman & Cowling (1939)), a point probability density function (pdf) $f_p^{(1)}(\mathbf{c}_p; \mathbf{x}_p, t)$ which defines the local instantaneous probable number of particle centers with the given translation velocity $\mathbf{u}_p = \mathbf{c}_p$ may be defined. This function obeys a Boltzmann-type kinetic equation, which accounts for momentum exchange with the carrier fluid and for the influence of external force fields such as gravity and inter-particle collisions. Reynolds-averaged transport equations of the first moments (such as particle concentration, mean velocity and particle kinetic stress) may be derived directly by averaging from the pdf kinetic equation (Simonin (1996))

To derive local instantaneous Eulerian equations in dilute flows (without turbulence modification by the particles) Février *et al.* (2002) proposed to use an averaging over all dispersed-phase realizations conditioned by one carrier-phase realization. Such an averaging leads to a conditional pdf for the dispersed phase,

$$\tilde{f}_p^{(1)}\left(\mathbf{c}_p; \mathbf{x}, t, H_f\right) = \left\langle W_p^{(1)}\left(\mathbf{c}_p; \mathbf{x}, t\right) | H_f \right\rangle. \tag{2.1}$$

$W_p^{(1)}$ are the realizations of position and velocity in time of any given particle (Reeks (1991)). With this definition one may define a local instantaneous particulate velocity field, which is here named "mesoscopic Eulerian particle velocity field". This field is obtained by averaging the discrete particle velocities measured at a given position and time for all particle-flow realizations and one given carrier-phase realization,

$$\tilde{u}_p\left(\mathbf{u}, t, H_f\right) = \frac{1}{\tilde{n}_p^{(1)}} \int \mathbf{c}_p \tilde{f}_p^{(1)}\left(\mathbf{c}_p; \mathbf{x}, t, H_f\right) d\mathbf{c}_p. \tag{2.2}$$

Here

$$\tilde{n}_p^{(1)} = \int \tilde{f}_p^{(1)}\left(\mathbf{c}_p; \mathbf{x}, t, H_f\right) d\mathbf{c}_p \tag{2.3}$$

is the mesoscopic particle-number density. For simplicity, the dependence of the above variables on H_f is not shown explicitly. Application of the conditional-averaging procedure to the kinetic equation governing the particle pdf leads directly to the transport equations for the first moments of number density and mesoscopic Eulerian velocity,

$$\frac{\partial}{\partial t}\tilde{n}_p + \frac{\partial}{\partial x_i}\tilde{n}_p \tilde{u}_{p,i} = 0 \tag{2.4}$$

$$\tilde{n}_p \frac{\partial}{\partial t}\tilde{u}_{p,i} + \tilde{n}_p \tilde{u}_{p,j}\frac{\partial}{\partial x_j}\tilde{u}_{p,i} = -\frac{\tilde{n}_p}{\tilde{\tau}_p^F}\left[\tilde{u}_{p,i} - u_{f,i}\right] - \frac{\partial}{\partial x_j}\tilde{n}_p \delta\tilde{\sigma}_{p,ij} + \tilde{n}_p g_i. \tag{2.5}$$

Here $\delta\tilde{\sigma}_{p,ij}$ is the mesoscopic kinetic stress tensor of the particle Quasi-Brownian velocity distribution.

The current objective is to show that this term is non-negligible for inertial particles in turbulent flow.

2.1. *The stress tensor of quasi-Brownian motion (QBM)*

The stress term in (2.5) arises from an ensemble average of the nonlinear term in the transport equation for particle momentum,

$$\tilde{n}_p \delta\tilde{\sigma}_{p,ij} = \int (c_{p,i} - \tilde{u}_{p,i})\,(c_{p,j} - \tilde{u}_{p,j})\,\tilde{f}_p^{(1)}\,(\mathbf{c}_p; \mathbf{x}, t, H_f)\,d\mathbf{c}_p \tag{2.6}$$

$$= \tilde{n}_p \delta u_{p,i}\widetilde{\delta u_{p,j}}. \tag{2.7}$$

When the Euler or Navier-Stokes equations are derived from kinetic gas theory the trace of $\delta u_{p,i}\widetilde{\delta u_{p,j}}$ is interpreted as temperature (ignoring the Boltzmann constant and molecular mass) and related to pressure by an equation of state. In the case of the Euler or Navier-Stokes equations temperature is defined as the uncorrelated part of the kinetic energy. Here the uncorrelated part of the particulate kinetic energy is defined as

$$\delta q_p^2 = \frac{1}{2}\delta u_{p,i}\widetilde{\delta u_{p,i}}. \tag{2.8}$$

In analogy to the Euler or Navier-Stokes equations a quasi-Brownian pressure (QBP) may be defined by the product of uncorrelated kinetic energy and particle number density, as

$$\tilde{P}_p = \tilde{n}_p \frac{2}{3}\delta q_p^2 \tag{2.9}$$

When the particle number distribution becomes nonuniform, as in the case of a compressible gas, this pressure term tends to homogenize particle number density.

The non-diagonal part of the stress tensor can be identified, in analogy to the Navier Stokes equations, as a viscous term ($\theta_{p,ij}$). The momentum-transport equation (2.5) becomes

$$\tilde{n}_p \frac{\partial}{\partial t}\tilde{u}_{p,i} + \tilde{n}_p \tilde{u}_{p,j}\frac{\partial}{\partial x_j}\tilde{u}_{p,i} = -\frac{\tilde{n}_p}{\tilde{\tau}_p^F}\left[\tilde{u}_{p,i} - \tilde{u}_{f,i}\right] - \frac{\partial}{\partial x_i}\tilde{P}_p + \frac{\partial}{\partial x_j}\theta_{p,ij} + \tilde{n}_p g_i. \tag{2.10}$$

Furthermore it can be shown mathematically (Le Veque (1996)) that (2.10) without a pressure-like term leads to non physical solutions characterised by "shock"-like fronts in number density.

2.2. *Simulations without and with QBM*

First, preliminary simulations were performed without any stress term related to QBM. Particles tend to accumulate rapidly in small regions, causing unphysically high number densities. This causes the numerical simulation to fail. In order to ensure that failure was not due to a numerical problem, different simulations with different turbulence Reynolds numbers and Stokes numbers were performed, leading to the same result.

Simulations with a quasi-Brownian pressure (QBP) and without quasi-Brownian viscous stress were performed on the same test cases. Février *et al.* (2002) measured, in forced homogeneous isotropic turbulence, a mean quasi-Brownian kinetic energy $\langle \delta q_p^2 \rangle$ proportional to the mean mesoscopic kinetic energy $\tilde{q}_p^2 = \frac{1}{2}\langle \tilde{u}_{p,i}\tilde{u}_{p,i} \rangle$ with a proportionality coefficient depending on the Stokes number. Here a simple relation between the quasi-Brownian kinetic energy δq_p^2 needed in the QBP equation (2.9) and the mean resolved kinetic energy $\tilde{q}_p^2$ was used:

$$\delta q_p^2 = 5 * \tilde{q}_p^2. \tag{2.11}$$

Such a QBP modeling allows all the test cases that failed without a quasi-Brownian

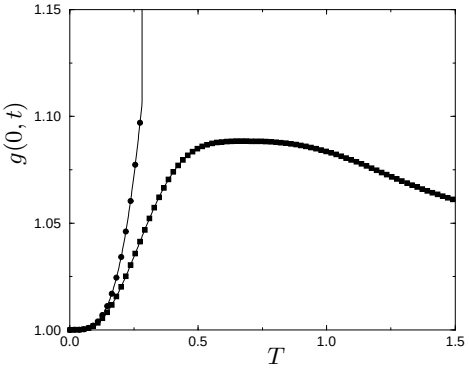

FIGURE 1. Segregation of the dispersed phase with QBP —■— , without QBP —●— .

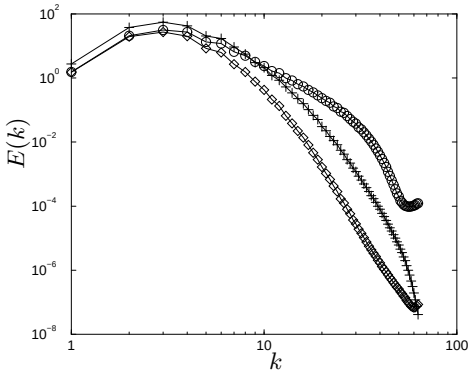

FIGURE 2. non-dimensional spectra of a test case ($128^3, Re = 42$) carrier phase + , dispersed phase without QBM ○ , dispersed phase with QBM ◇ .

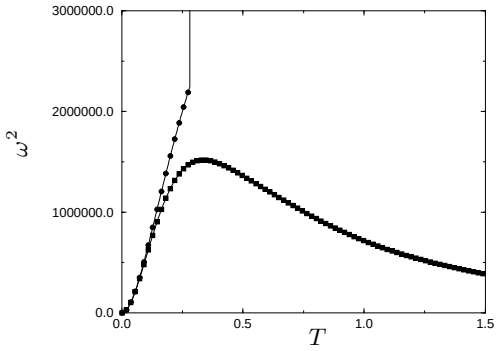

FIGURE 3. Enstrophy of the dispersed phase: with QBP —■— , without QBP —●— .

stress term to be simulated. But, compared to the value found by Février *et al.* (2002), relation (2.11) strongly overestimates the quasi-Brownian kinetic energy and so the effect of QBP. The need for such a large pressure term to carry out the simulation is probably due to the fact that the viscous-stress term is neglected.

In order to quantify the effect of particle segregation, the normalized variance of particle number density is introduced:

$$g(r,t) = \frac{\langle n(x,t)n(x+r,t)\rangle}{\langle n(x,t)\rangle^2} \tag{2.12}$$

figure 1 compares the time evolution of $g(0,t)$ from simulations with and without QBP. The quasi-Brownian pressure is found to limit the particle segregation effect to reasonable values.

figure 2 compares the kinetic energy spectra of the carrier phase and the dispersed phase with and without QBP. When simulations are performed without QBP, particle kinetic energy for small scales becomes larger then the carrier-phase kinetic energy in contrast with available results (Février *et al.* (2002)). This effect increases in time and can

be characterized by the temporal increase of the particle enstrophy as shown by figure 3. This is probably due to the unphysically large accumulation of particles in specific regions of the carrier phase turbulent flow (regions of high strain and low vorticity). Indeed, when accounting for the QBP contribution limiting segregation, the particle enstrophy behavior looks much more reasonable. The quasi-Brownian viscous stress should also play an important role by inducing a strong dissipative effect to the small scales in addition to the one due to the drag force.

2.3. *Measurement of particle dispersion*

Particle dispersion is usually measured in Lagrangian simulations by tracking individual particle path and calculating the variance of the relative displacement

$$\left\langle X_p^2(t)\right\rangle = \frac{1}{N}\sum_{j=1}^{N}\left[x_{p,j}(t) - x_{p,j}(t_0)\right]^2. \tag{2.13}$$

Particle dispersion can then be related to the time derivative of this quantity (see Monin & Yaglom (1987)),

$$D_p^L(t) = \frac{1}{2}\frac{d}{dt}\left\langle X_p^2(t)\right\rangle. \tag{2.14}$$

In Eulerian simulations one does not have access to individual particle paths. Particle dispersion can still be measured by a semi-empirical method (Monin & Yaglom (1987)): Suppose that the simulation is being carried out with colored particles and a transport equation is written for the ratio of colored particles to total particles ($\tilde{c} = \tilde{n}_c/\tilde{n}_p$). This transport equation is similar to the transport equation for particle number density (2.4):

$$\frac{\partial}{\partial t}\tilde{c}\tilde{n}_p + \frac{\partial}{\partial x_i}\tilde{c}\tilde{n}_p\tilde{u}_{p,i} = \frac{\partial}{\partial x_i}\tilde{c}\tilde{n}_p\left(\tilde{u}_{p,i} - \tilde{u}^c_{p,i}\right) \tag{2.15}$$

Here, $\tilde{u}^c_{p,i}$ is the mesoscopic velocity of colored particles. Since only the velocity of the total droplet number is resolved, a supplementary term arises on the right-hand side of (2.15). This term takes into account the slip velocity between colored particles and the mesoscopic velocity of the particle ensemble. Comparing the above equation to the Navier-Stokes equations, this term is the equivalent of molecular diffusion in a species equation. Since the slip velocity can arise only from uncorrelated movement of the particles, this term can be modeled as a diffusion related to the quasi-Brownian motion.

If the ensemble-averaged mean number-density fraction of colored particles $\langle\tilde{n}_p\rangle\,\mathcal{C} = \langle\tilde{n}_p\tilde{c}\rangle$, ($\tilde{c} = \mathcal{C} + c'$) is uniformly stratified, say in the k-direction, and fluctuations are assumed periodic with respect to the computational domain, the fluctuating number density of colored particles $c'\tilde{n}_p$ can be extracted from the total colored number density and one obtains a transport equation for the fluctuations of colored-particle concentration:

$$\frac{\partial}{\partial t}c'\tilde{n}_p + \frac{\partial}{\partial x_i}c'\tilde{n}_p\tilde{u}_{p,i} = -\tilde{n}_p\tilde{u}_{p,k}\frac{\partial}{\partial x_k}\mathcal{C} + \frac{\partial}{\partial x_i}\tilde{c}\tilde{n}_p(\tilde{u}_{p,i} - \tilde{u}^c_{p,i}) \tag{2.16}$$

Averaging the colored number-density equation ((2.15)) one obtains a Reynolds-averaged transport equation,

$$\frac{\partial}{\partial t}\left\langle\tilde{n}_p\right\rangle\mathcal{C} + \frac{\partial}{\partial x_i}\left\langle\tilde{n}_p\right\rangle\mathcal{C}\left\langle\tilde{u}_{p,i}\right\rangle_p = -\frac{\partial}{\partial x_i}\left\langle\tilde{n}_p c' u_{p,i}\right\rangle + \frac{\partial}{\partial x_i}\left\langle\tilde{c}\tilde{n}_p\left(\tilde{u}_{p,i} - \tilde{u}^c_{p,i}\right)\right\rangle. \tag{2.17}$$

Equation 2.16 has been solved neglecting the quasi Brownian motion term. Particle dispersion can be derived by making a gradient assumption: ($\langle c'\tilde{n}_p\tilde{u}_{p,k}\rangle = \langle\tilde{n}_p\rangle\, D^t_{p,k}\frac{\partial}{\partial x_k}\mathcal{C}$)

A semi-empirical diffusion coefficient is defined by:

$$D^t_{p,k} = \frac{\langle \tilde{n}_p c' u_{p,k} \rangle}{\langle \tilde{n}_p \rangle \frac{\partial}{\partial x_k} \mathcal{C}} \tag{2.18}$$

This dispersion coefficient is comparable to the Lagrangian dispersion coefficient (2.14) in the long-time limit of stationary turbulence. Nevertheless simulations neglecting the quasi-Brownian motion are likely to underestimate the Lagrangian dispersion.

3. Numerical implementation

The Eulerian equations for the dispersed phase have been implemented into the Navier-Stokes Solver AVBP (Schönfeld & Rudyard (1999)). It is based on a 2D/3D finite Volume/ finite Element method for unstructured, structured and hybrid meshes.

4. Description of the test case

Particle dynamics and particle dispersion have been studied by experiments and by Lagrangian computations. One appealing test case is that of Snyder & Lumley (1971) (hereafter referred to as SL). They inserted particles with different inertial properties into grid generated spatially decreasing turbulence and measured particle dynamics as well as particle dispersion. This test case has been computed with a Lagrangian approach by Elghobashi & Truesdell (1992) (from heron referred to as ET). The carrier phase was taken as a temporarily decreasing homogeneous isotropic turbulence corresponding to the grid generated turbulence of SL. After an initial calculation for two turnover times ($t = l_{ii}/u'_f$), particles were inserted. Analysis of particle dynamics as well as dispersion was carried out by ET on particles corresponding to those of SL, and a direct comparison was made. Here the procedure of ET is followed, but the calculation is performed by an Eulerian-Eulerian approach and a comparison with the experimental results of SL and the Lagrangian computation of ET is attempted. The present numerical simulation was performed on a periodic 128^3 grid.

4.1. *Initialization of the homogeneous isotropic turbulence*

The carrier-phase velocity field is initialized at dimensionless time $T = 0$ with a divergence-free velocity field such that the kinetic energy satisfies the spectrum (Elghobashi & Truesdell (1992)):

$$E(k,0) = \frac{3}{2} u'^2_{f,0} \frac{k}{k_p} \exp\left(-\frac{k}{k_p}\right) \tag{4.1}$$

where u'_f is the dimensionless rms velocity, k is the wavenumber and k_p is the wavenumber of peak energy. All wave numbers are normalized by the minimal wavenumber k_{min}. In the present simulation the values of ET were taken. Properties of the carrier-phase turbulence are validated against the properties of carrier-phase turbulence of SL and ET. The spatial evolution of the flow in the experiment of SL is converted to a temporal evolution of the flow by $t = x/\bar{U}$. Here $\bar{U}$ is the mean convection velocity in the experiment.

In figure 4 the dimensionless velocity square u'^2_f of the carrier phase is compared to experiment (SL) and Lagrangian simulation (ET). Since the temporally-decaying turbulence was chosen with the same initial parameters as that of ET, it has the same decay behavior.

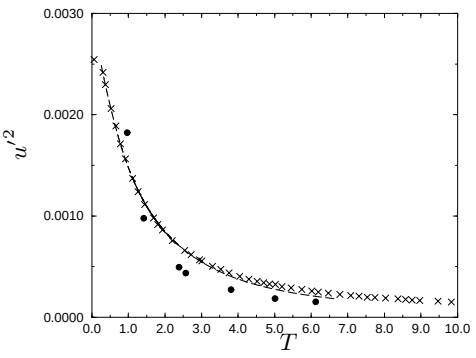

FIGURE 4. Evolution of dimensionless carrier phase $u_f'^2$ for experiment (SL) • , Lagrangian simulation (ET) × , and present simulation – – – –

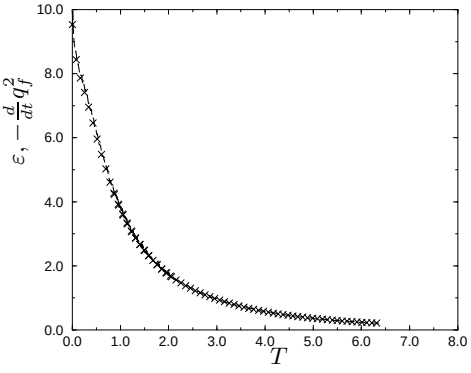

FIGURE 5. Comparison of dissipation ε – – – – with change of kinetic energy $-\frac{d}{dt}q_f^2$ × of the carrier phase in the present simulation.

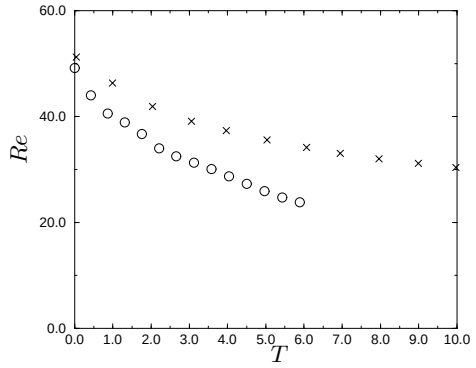

FIGURE 6. Evolution of carrier phase Reynolds number Lagrangian simulation (ET) Re_l × , and present simulation Re_l ○ .

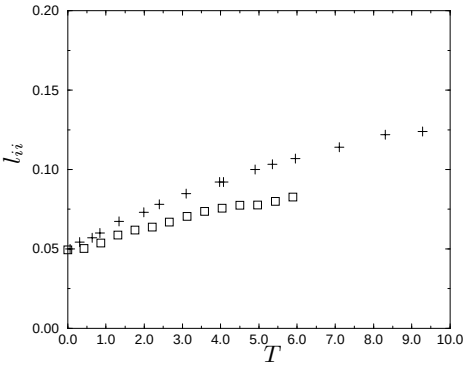

FIGURE 7. Evolution of integral length scale l for the Lagrangian simulation (ET) + , and present simulation □ .

To verify numerical resolution, dissipation ε is compared to temporal change of kinetic energy $\frac{d}{dt}q_f^2$ in figure 5. It shows excellent agreement between calculated dissipation and kinetic energy decrease. Therefore it can be assumed that numerical dissipation is negligible compared to viscous dissipation.

In figure 6 the Reynolds number of the present simulation is compared to the Lagrangian simulation (ET). In the present simulation the turbulent Reynolds number (based on integral length scale) decays more rapidly compared to the simulation of ET. This is due to the slower temporal increase of the integral length scale (figure 7) in the present simulation.

4.2. *Particle properties and initialization*

The Eulerian-Eulerian simulation was performed with one-way coupling. Therefore the carrier-phase turbulence had no feedback from the dispersed phase. The only interaction force taken into account in the momentum equation of the dispersed phase was drag. This is justified in the limit of large density ratios (ρ_p/ρ_g). The characteristic particle

	hollow glass	corn pollen	solid glass	copper
d $[m]$	$4.65*10^{-5}$	$8.7*10^{-5}$	$8.7*10^{-5}$	$4.65*10^{-5}$
density ratio (ρ_p/ρ_f)	260	1000	2500	8900
Re_d	0.25	0.47	0.47	0.25
initial τ_p (SL) $[s]$	0.0055	0.020	0.045	0.049
initial τ_p (ET) $[s]$		0.027	0.061	0.067
initial τ_p (non dimensional)	0.053	0.193	0.432	0.473
terminal velocity $v_{t,0}/u_0'$		3.16	6.69	7.57
St $(\tau_p/\tau_{f,0}$)	0.024	0.09	0.203	0.221

TABLE 1. Particle properties in experiment (SL), Lagrangian simulation (ET) and present simulation.

relaxation time is computed by the standard formulation.

$$\tau_p = \frac{\rho_p d^2}{18 f(Re_p)\mu} \tag{4.2}$$

$$f(Re_p) = 1 + 0.15 Re_p^{0.687 d0} \tag{4.3}$$

The particle Reynolds number for the drag force correction $f(Re_p)$ is based on the slip velocity $Re_p = (|\tilde{u}_p - u_f|\, d)/\nu_f$. For the present numerical simulation, particle properties are chosen such that they have the same particle Reynolds number $Re_d = (u' d)/\nu_f$ as in the experiment and the same Stokes number in terms of turnover time $St = \tau_p/\tau_{f,0}$ $(\tau_{f,0} = l_0'/u_0')$. † For the Eulerian-Eulerian simulation, particles corresponding to corn pollen or glass beads were retained. Particles were inserted as in the Lagrangian simulation (ET) at the dimensionless time $T = 2.0$. They were given the same velocity as the carrier phase in both simulations when inserted into the turbulent flow. In the Lagrangian simulation, particles had relaxed to the carrier-phase turbulence at $T = 2.67$ and evaluation of particle-dispersion statistics started at that time, corresponding to the equivalent particle-dispersion measurements of (SL). Particle properties were then analyzed in turbulence with and without gravity. When particles are subject to gravity they establish a mean terminal velocity in the direction of gravity, given by $v_t = g * \tau_p$. The gravity constant g was chosen such that the Eulerian-Eulerian simulation predicts the same ratio of $v_{t,0}/u_0'$ (see Tab. 1) as in the experiment and the Lagrangian simulations.

5. Particle dynamics

Particle dynamics are analyzed in simulations with and without gravity. In the publication of ET only the square of the relative velocity, not the total kinetic energy is given. In the publication of SL, on the other hand, only the square of the particle velocity given. Therefore those quantities are compared separately.

5.1. *Particle dynamics without gravity*

For both types of particles, corn pollen and glass beads, the relative square velocity in the present simulation shows the same qualitative behavior as in the Lagrangian simulation.

† The index $_0$ is used for values at the dimensionless time $T = 2.67$ as in SL.

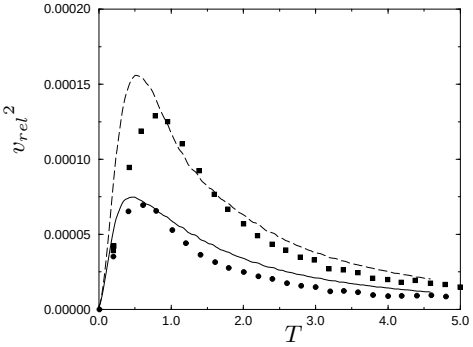

FIGURE 8. Evolution of dimensionless relative square velocity without gravity: Lagrangian simulation (ET) corn pollen ● , Lagrangian simulation (ET) glass beads ■ , present simulation corn pollen ——— , and present simulation glass beads - - - - .

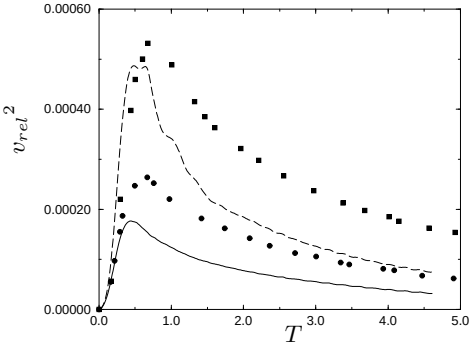

FIGURE 9. Evolution of dimensionless relative square velocity with gravity (perpendicular to gravity): Lagrangian simulation (ET) corn pollen ● , Lagrangian simulation (ET) glass beads ■ , present simulation corn pollen ——— , and present simulation glass beads - - - - .

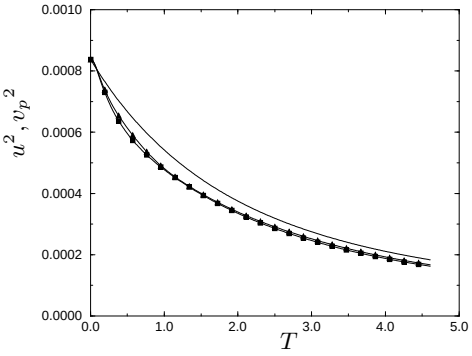

FIGURE 10. Evolution of dimensionless squared velocities without gravity in the present simulation: carrier phase ——— corn pollen —▲— , glass beads —■— .

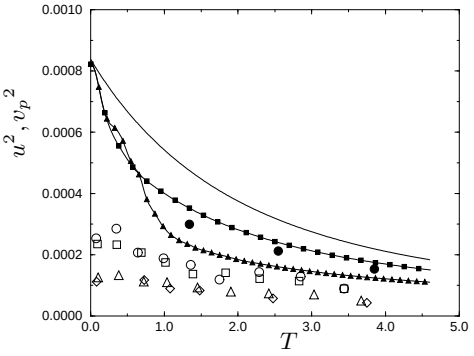

FIGURE 11. Evolution of dimensionless squared particle velocities (perpendicular to gravity) with gravity: experiment (SL) carrier phase ● , experiment (SL) hollow glass ○ , experiment (SL) corn pollen □ , experiment (SL) glass beads △ , experiment (SL) copper △ , present simulation carrier phase ——— , present simulation corn pollen —■— , and present simulation glass beads —▲— .

However the slip velocity is overestimated In both cases (figure 8). The Eulerian mean-square relative velocity $\tilde{v}_{rel}^2 = \left\langle (u_f - \tilde{u}_p)^2 \right\rangle$ differs from the Lagrangian mean-square relative velocity $v_{rel}^2 = \left\langle (u_f - u_p)^2 \right\rangle$ by the quantity δu_p^2, from QBM. Therefore the predicted Eulerian mean-square relative velocity should be lower than the Lagrangian mean-square relative velocity.

Fig. 10 shows the temporal development of the carrier phase $\left\langle u_f^2 \right\rangle$ and the square velocities of corn pollen and glass beads. Since both particles are in the same range of

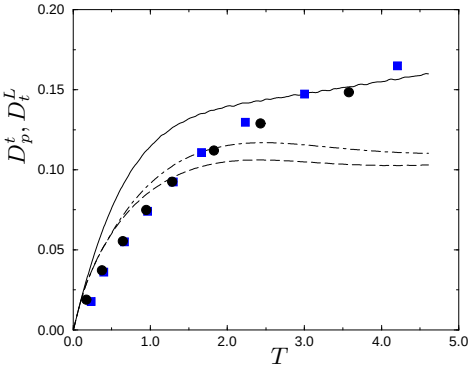

FIGURE 12. Evolution of the dispersion coefficient without gravity: Lagrangian simulation (ET) carrier phase ● , Lagrangian simulation (ET) corn pollen ■ , present simulation fluid particle ——— , present simulation corn pollen - - - - , and present simulation glass beads —·—

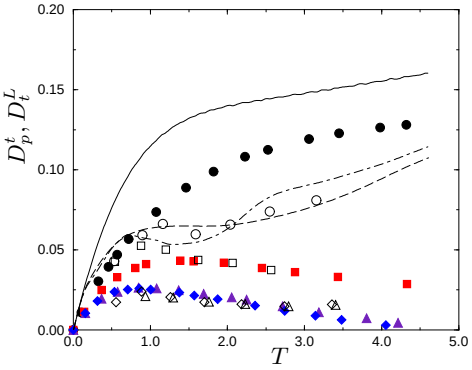

FIGURE 13. Evolution of the dispersion coefficient with gravity: experiment (SL) hollow glass ○ , experiment (SL) corn pollen □ , experiment (SL) glass beads △ , Lagrangian simulation (ET) carrier phase ● , Lagrangian simulation (ET) corn pollen ■ , present simulation carrier phase ——— , present simulation corn pollen - - - - , and present simulation glass beads —·—

Stokes numbers, the square velocities differ only very little. This quantity was not given by ET and can therefore not be compared.

5.2. *Particle dynamics with gravity*

As expected, when gravity is taken into account, particle dynamics are modified. Indeed, the crossing-trajectory effect due to the mean settling velocity of the particles leads to a decrease of the integral time scale of the fluid turbulence viewed by the particles. Such an effect leads to an increase of the effective particle Stokes number and so to an increase of the relative squared velocity with respect to the non-settling case, as shown by figure 9.

After about one turnover time particle square velocity perpendicular to gravity shows qualitatively similar behavior as the experimental values of SL (figure 11). The predicted particle square velocity is larger than the measured one. This may be due to the fact that simulated carrier phase $< u_f^2 >$ is also higher than the experimental value.

6. Particle dispersion

Particle dispersion is measured as explained in section 2.3 for the dispersed phase. In order to compare with the carrier phase, the equivalent of (2.16) is solved for the carrier phase without molecular diffusion. As in the work of ET, dispersion coefficients are normalized by the integral length scale at $T = 2.67$.

6.1. *Particle dispersion without gravity*

Figure 12 shows the evolution of the Lagrangian and Eulerian dispersion coefficient in the simulations without gravity. ET calculated the Lagrangian dispersion without gravity only for the carrier phase and corn pollen. In the Eulerian simulation the carrier phase shows the same qualitative behavior as the Lagrangian simulation of ET, but the dispersion of corn pollen is lower then the dispersion of the carrier phase. As discussed previously (section. 2.3) this might be due to the missing QBM part of the dispersion.

6.2. *Particle dispersion with gravity*

In the Eulerian simulations with gravity, particle dispersion is significantly lower then in the simulations without gravity, consistent with the Csanady (1963) analysis. This observation matches the Lagrangian simulation. Quantitatively, however, dispersion measured in the Eulerian simulations is high compared to Lagrangian simulations.

7. Conclusion

In the first part of this paper it was shown that unsteady Eulerian-Eulerian simulations need to take into account the stress tensor related to the uncorrelated quasi-Brownian motion in the case of inert particles. It is not clear how this term needs to be handled in more complex LES computations, and further investigation of this term is necessary.

In the second part, a preliminary model for QBM was used by relating unresolved particle kinetic energy to the resolved particle kinetic energy by a fixed coefficient. This model allowed simulations to be performed for the experiment of Snyder & Lumley (1971) and to compare the results to the Lagrangian simulations of Elghobashi & Truesdell (1992). Even if the numerical results of the Eulerian simulation do not quantitatively match the Lagrangian simulations exactly, this test showed that Eulerian simulations could be an alternative tool for simulations of dispersed two-phase flows.

REFERENCES

Chapman, S., & Cowling, T.G. 1939 *The Mathematical Theory of Non-Uniform Gases.* Cambridge University Press.

Csanady, G.T. 1963 Turbulent diffusion of heavy particles in the atmosphere. *J. Atmos. Sci.* **20**, 201–208.

Drew, D.A. & Passman, S.L. 1998 *Theory of Multicomponent Fluids.* Springer Series in Applied Mathematical Sciences vol. 135.

Druzhini, O.A. & Elghobashi, S. 1999 On the decay rate of isotropic turbulence laden with micro-particles. *Phys. Fluids* **11**, 602–610.

Elghobashi, S. & Truesdell, G.C. 1992 Direct simulation of particle dispersion in a decaying isotropic turbulence. *J. Fluid Mech.* **242**, 655–700.

Février P. & Simonin, O. 2000 Statistical and continuum modeling of turbulent reactive particulate flows. *VKI Lecture Series* 2000-06.

Février, P. 2000 Etude numerique des effets de concentration preferentielle et de correlation spatiale entre vitesses des particles solides en turbulence homogene isotrope stationaire. *PhD Thesis*, INP, Toulouse.

Février, P., Simonin, O. & Squires, K. D. 2002 On the continous field and quasi-Brownian distribution of particle velocities in turbulent flows: theoretical formalism and numerical study. Submitted to J. Fluid. Mech.

Fuchs, N. A. 1964 *The Mechanics of Aerosols.* Dover, Mineola, NY.

Le Veque, R. J. 1996 *Numerical Methods for Conservation Laws.* Birkhäuser, Boston.

Monin, A. S. & Yaglom, A. M. 1987 *Statistical Fluid Mechanics*, Vol. 1 MIT Press, Cambridge, MA.

Reeks M. W. 1991 On a kinetic equation for the transport of particles in turbulent flows *Phys. Fluids A* **3**, 446–456.

Snyder, W. H. & Lumley, J. L. 1971 Some measurements of particle velocity auto-correlation functions in a turbulent flow. *J. Fluid Mech.* **48**, 41–71.

Schönfeld, T. & Rudyard, M. 1999 Steady and unsteady flow simulations using the hybrid flow solver AVBP. *AIAA J.* **37**, 1378–1385.

Simonin, O., Février, P. & Lavieville, J. 2002 On the spatial distribution of heavy particle velocities in turbulent flow: From continuous field to particulate chaos. *Journal of Turbulence* **Vol 3**, 40.

Simonin, O. 1996 Combustion and turbulence in two-phase flows *VKI Lecture Series* 1996-02.